

Dynamic Analysis of Large-Scale Mechanical Systems and Animated Graphics

Parviz E. Nikravesh*
University of Iowa, Iowa City, Iowa

This paper presents a computer-based method for formulation and solution of coupled differential and algebraic equations describing large-scale mechanical systems, including feedback control, aerodynamic forces, and other multidisciplinary effects that interact with the mechanical system. A Euler parameter representation of the configuration of the mechanical system is employed to obtain singularity free solution for generalized coordinates and a much simplified algebraic formulation of the governing system of equations, compared with the more classical Euler angle generalized coordinate formulation. A generalized coordinate partitioning algorithm is employed to identify independent generalized coordinates automatically and reduce the dimension of the numerical integration problem. Animated graphics output is employed to assist in visualization of dynamic performance of several systems—a parachute descending in air, an aircraft landing on a damaged runway, and a truck with flexible chassis.

Introduction

THE field of computer aided dynamic analysis of mechanisms and machines has seen substantial development during the past decade, with introduction of planar system dynamic codes^{1,2} and, more recently, general purpose spatial system dynamic simulations.^{3,4} These codes treat rigid body mechanism and machine dynamics and have not been extended to incorporate interdisciplinary aspects of large-scale dynamic systems. In this respect, the field of mechanical system dynamics substantially lags behind the better developed fields of electrical circuit analysis, and especially behind the well developed field of finite element structural analysis.

The computer based system dynamic analysis technique presented in this paper has been developed^{5,6} with the objective of automated generation of the governing equations for constrained dynamic systems and coupled with differential and algebraic equations representing feedback control subsystems, hydraulic subsystems, vehicle power plants, aerodynamic forces, and other interacting subsystems that make up modern automotive and industrial equipment. While the development here is limited to mechanical systems composed of rigid bodies, a recent development allows for direct extension of the technique and of a computer code to incorporate effects of flexibility of elastic bodies making up the mechanical systems.^{7,8} In this paper, kinematic constraint equations are assumed to be holonomic. However, the algorithm can be generalized to accept holonomic and nonholonomic equations.⁹

Mechanical System Representation

In order to specify the position of a rigid body in an inertial (global) x - y - z coordinate system, it is sufficient to specify the spatial location of the origin and the angular orientation of a ξ - η - ζ coordinate system that is rigidly attached to the body. In this paper, coordinate rotations are defined by Euler parameter generalized coordinates.¹⁰

Euler Parameter Generalized Coordinates

Let the ξ - η - ζ axes be attached to the i th body of the system, as shown in Fig. 1, where the origin O_i is located at the center of mass of the body. A point P on body i is located in the inertial coordinate system by

$$\mathbf{r}_i^P = \mathbf{r}_i + \mathbf{A}_i \mathbf{s}_i'^P \quad (1)$$

where $\mathbf{s}_i'^P \equiv [\xi^P, \eta^P, \zeta^P]^T$ are the coordinates of P in the ξ - η - ζ coordinate system, $\mathbf{r}_i \equiv [x, y, z]^T$ are the coordinates of O_i in the x - y - z coordinate system, and \mathbf{A}_i is the rotational transformation matrix of body i . Matrix \mathbf{A}_i , expressed in terms of Euler parameters e_{0i} , e_{1i} , e_{2i} , and e_{3i}

$$\mathbf{A}_i = 2 \begin{bmatrix} e_0^2 + e_1^2 - 1/2 & e_1 e_2 - e_0 e_3 & e_1 e_3 + e_0 e_2 \\ e_1 e_2 + e_0 e_3 & e_0^2 + e_2^2 - 1/2 & e_2 e_3 - e_0 e_1 \\ e_1 e_3 - e_0 e_2 & e_2 e_3 + e_0 e_1 & e_0^2 + e_3^2 - 1/2 \end{bmatrix}_i \quad (2)$$

where the four Euler parameters are required to satisfy the equation

$$\mathbf{e}_0^2 + \mathbf{e}^T \mathbf{e} = e_0^2 + e_1^2 + e_2^2 + e_3^2 = 1 \quad (3)$$

The vector of parameters $\mathbf{e} \equiv [e_1, e_2, e_3]^T$ are the x - y - z (or ξ - η - ζ) components of a vector lying on the axis of rotation about which the body can be rotated from a reference position (in which the x - y - z and ξ - η - ζ axes are parallel) to the current position, as shown in Fig. 2. The vector \mathbf{e} is defined by

$$\mathbf{e} = u \sin \chi / 2 \quad (4)$$

where u is a unit vector on the axis of rotation and χ is the angle of rotation. Existence of the axis is assured by Euler's theorem.¹⁰ The fourth parameter e_0 is defined as

$$e_0 = \cos \chi / 2 \quad (5)$$

Constraint Equations

Standard constraints between rigid bodies are taken as friction-free (workless) joints. Formulations for two con-

Presented as Paper 83-0946 at the AIAA/ASME/ASCE/AHS Structures, Structural Dynamics and Materials Conference, Lake Tahoe, Nev., May 2-4, 1983; received May 12, 1983; revision received Jan. 13, 1984. Copyright © American Institute of Aeronautics and Astronautics, Inc., 1984. All rights reserved.

*Assistant Professor, Mechanical Engineering.

straints are presented here as follows:

Spherical Joint

Figure 3 shows two adjacent bodies i and j connected by a spherical joint (ball joint). A vector loop equation can be written as

$$\mathbf{r}_i + \mathbf{s}_i - \mathbf{s}_j - \mathbf{r}_j = \mathbf{0} \quad (6)$$

Using Eq. 1, this equation can be rewritten as

$$\mathbf{r}_i + A_i \mathbf{s}_i^P - \mathbf{r}_j - A_j \mathbf{s}_j^P = \mathbf{0} \quad (7)$$

where the center P of the ball joint is located by the body-fixed vectors \mathbf{s}_i^P and \mathbf{s}_j^P in bodies i and j , respectively.

Revolute Joint

Figure 4 depicts a revolute joint between bodies i and j . Point P is common to both bodies and points Q_i and Q_j are located on bodies i and j , respectively, defining the axis of

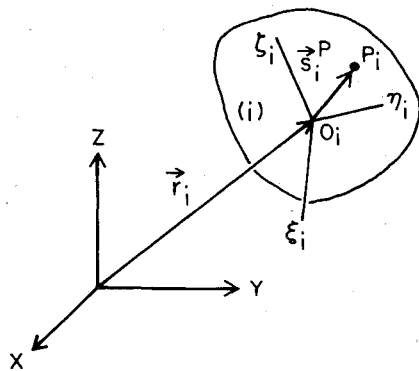


Fig. 1 Body-fixed ξ_i - η_i - ζ_i and global x - y - z coordinate systems.

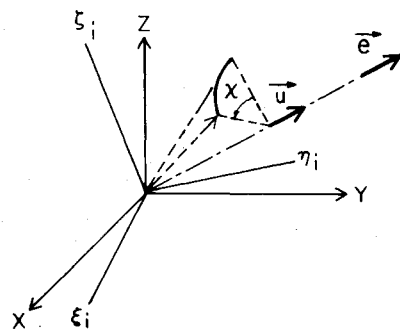


Fig. 2 Angular rotation of ξ_i - η_i - ζ_i coordinate system about \vec{u} axis.

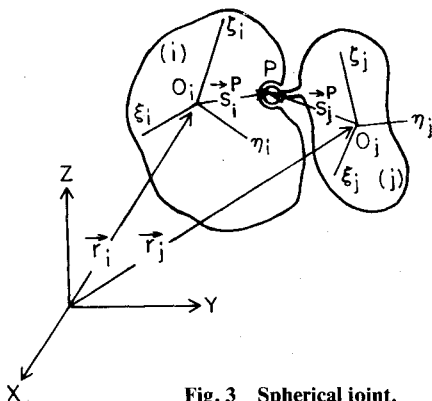


Fig. 3 Spherical joint.

rotation of the joint. Equation (7) also holds for this joint. Additional constraints are obtained by requiring the cross product of vectors \mathbf{g}_i and \mathbf{g}_j to be zero, which forces the points P , Q_i , and Q_j to lie on a common line. Vectors \mathbf{g}_i and \mathbf{g}_j can be expressed in component form as

$$\mathbf{g}_k \equiv A_k (\mathbf{s}_k^Q - \mathbf{s}_k^P), \quad k=i, j \quad (8)$$

Then, the cross product of \mathbf{g}_i and \mathbf{g}_j , set equal to zero, yields three scalar equations

$$\tilde{\mathbf{g}}_i \mathbf{g}_j = \mathbf{0} \quad (9)$$

where $\mathbf{g}_i = [u, v, w]^T$, and $\tilde{\mathbf{g}}_i$ is a skew-symmetric matrix containing the components of \mathbf{g}_i , defined as

$$\tilde{\mathbf{g}}_i \equiv \begin{bmatrix} 0 & -w & v \\ w & 0 & -u \\ -v & u & 0 \end{bmatrix}_i$$

Of the three scalar equations of Eq. (9), only two are independent. The best two should be selected, along with Eq. (7), to form five constraint equations for the revolute joint.

Numerous other standard joints may be formulated in the same way⁶ including cylindrical, universal, translational, screw, and composite joints. Once each of the standard joints is defined algebraically, the composite set of joint equations of a large-scale system can be automatically assembled. This approach is analogous to assembling a finite-element model of a structure from element stiffness and mass matrices.

Equations of Rigid Body Dynamics

For body i , let $\omega_i' = [\omega_{\xi}, \omega_{\eta}, \omega_{\zeta}]^T$ be the projection of the angular velocity vector onto the local coordinate axes, $\mathbf{r}_i = [x, y, z]^T$ be the global location of the center of mass, m_i be the mass and $j_{\xi\xi}, j_{\eta\eta}, j_{\zeta\zeta}, j_{\xi\eta}, j_{\eta\xi}, j_{\xi\zeta}, j_{\zeta\xi}$ be the moments and products of inertia about the ξ_i, η_i , and ζ_i axes. The kinetic energy of the i th body can be written as¹¹

$$T_i = \frac{1}{2} \mathbf{r}_i^T N_i \dot{\mathbf{r}}_i + \frac{1}{2} \omega_i'^T J_i \omega_i' \quad (10)$$

where

$$N_i = \begin{bmatrix} m & 0 & 0 \\ 0 & m & 0 \\ 0 & 0 & m \end{bmatrix}_i, \quad J_i = \begin{bmatrix} j_{\xi\xi} & j_{\xi\eta} & j_{\xi\zeta} \\ j_{\eta\xi} & j_{\eta\eta} & j_{\eta\zeta} \\ j_{\zeta\xi} & j_{\zeta\eta} & j_{\zeta\zeta} \end{bmatrix}_i$$

Angular velocity ω_i' , in terms of Euler parameters, can be expressed as^{6,10}

$$\omega_i' = 2 \mathbf{G}_i \dot{\mathbf{p}}_i \quad (11)$$

where $\mathbf{p}_i \equiv [e_0, e_1, e_2, e_3]^T$ and

$$\mathbf{G}_i = \begin{bmatrix} -e_1 & e_0 & e_3 & -e_2 \\ -e_2 & -e_3 & e_0 & e_1 \\ -e_3 & e_2 & -e_1 & e_0 \end{bmatrix}_i \quad (12)$$

To simplify notation, let the kinematic constraint equations of all joints in the system, and n constraints of Eq. (3), be written in the form

$$\Phi(\mathbf{r}_i, \mathbf{p}_1, \mathbf{r}_2, \mathbf{p}_2, \dots, \mathbf{r}_n, \mathbf{p}_n, t) = \mathbf{0} \quad (13)$$

where Φ is an m -vector of functions of the generalized coordinates of the n bodies making up the system.

Lagrange's equations of motion for the i th body may now be written as¹¹

$$\frac{d}{dt} (T_{i_{\dot{r}_i}})^T + \phi_{r_i}^T \lambda - f_i = 0 \quad (14)$$

$$\frac{d}{dt} (T_{i_{\dot{p}_i}})^T - T_{i_{p_i}}^T + \phi_{p_i}^T \lambda - b_i = 0 \quad (15)$$

where f_i and b_i are the vectors of generalized forces and torques corresponding to generalized coordinates r_i and p_i , respectively. Subscripts denote partial differentiation and λ is a vector of Lagrange multipliers corresponding to the constraints. It is well known¹¹ that the Lagrange multipliers define the joint reaction forces.

Substitution of Eq. (10), with

$$T = \sum_{i=1}^n T_i$$

into Eqs. (14) and (15) yields

$$N_i \ddot{r}_i + \Phi_{r_i}^T \lambda = f_i \quad (16)$$

$$4G_i^T J_i G_i \ddot{p}_i + \Phi_{p_i}^T \lambda = b_i + 8\dot{G}_i^T J_i \dot{G}_i \dot{p}_i \quad (17)$$

Defining $g_i = [f_i^T, b_i^T + 8p^T \dot{G}^T J \dot{G}]^T$ and

$$M_i = \begin{bmatrix} N & 0 \\ 0 & 4G^T J G \end{bmatrix}_i \quad (18)$$

Equations (16) and (17) can be written as

$$M_i \ddot{q}_i = g_i - \Phi_{q_i}^T \lambda, \quad i = 1, \dots, n \quad (19)$$

where $q_i = [r_i^T, p_i^T]^T = [x, y, z, e_0, e_1, e_2, e_3]^T$. The total system equations of motion for n rigid bodies is then

$$M \ddot{q} = g - \Phi_q^T \lambda \quad (20)$$

and the algebraic equations of Eqs. (3) and (13), where $M = \text{diag. } [M_1, M_2, \dots, M_n]$, $g = [g_1^T, g_2^T, \dots, g_n^T]^T$, and $q = [q_1^T, q_2^T, \dots, q_n^T]^T$. This is a nonlinear system of differential-algebraic equations.

Forces of Spring-Damper-Actuators

Internal forces acting between bodies due to the action of springs, dampers, and actuators may be obtained by a process similar to the constraint equation development. For example, since springs, dampers, and actuators generally appear together, as shown in Fig. 5, they are incorporated into a single set of equations. Let the global coordinates of the attachment points be r_i^P and r_j^P . The length of the spring-damper-actuator is thus

$$\ell = \{ [r_i^P - r_j^P]^T [r_i^P - r_j^P] \}^{1/2} \quad (21)$$

The magnitude of the spring-damper-actuator force is

$$f = k(\ell - \ell^0) + c\dot{\ell} + a \quad (22)$$

where ℓ^0 is the undeformed length of the spring, $\dot{\ell}$ is the time rate of change of the spring length ℓ , and k , c , and a are the spring rate, damping coefficient, and actuator force, respectively. The force and torque components of each spring-damper-actuator element in the system are added to the generalized force vector g of Eq. (20).⁶

Similar to the translational spring-damper-actuator, torsional spring-damper-actuator elements may be defined

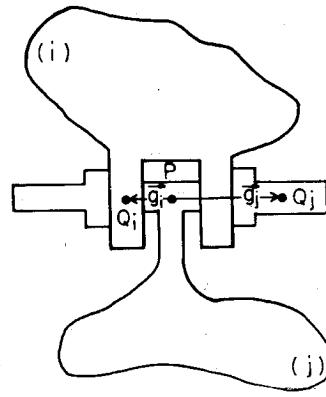


Fig. 4 Revolute joint.

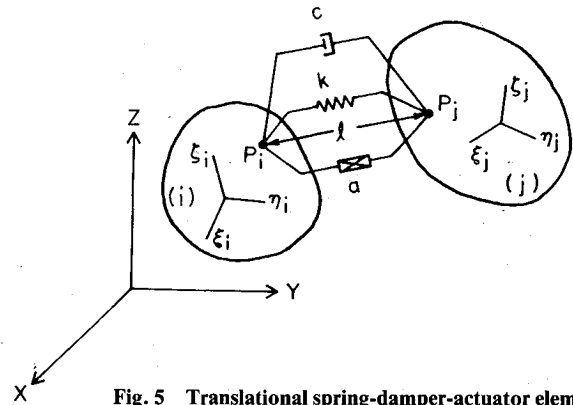


Fig. 5 Translational spring-damper-actuator element.

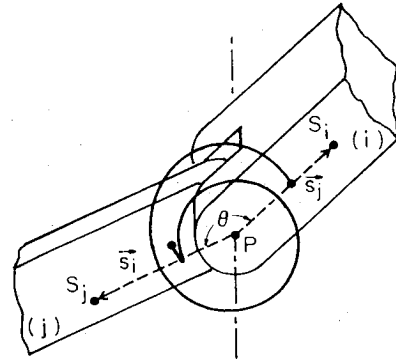


Fig. 6 Torsional spring-damper-actuator element.

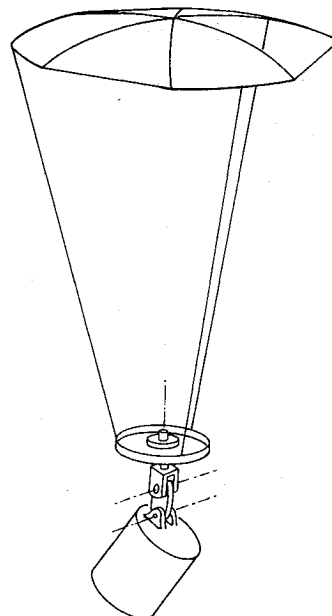


Fig. 7 Parachute model.

between adjacent bodies i and j that are connected by a revolute joint, as shown in Fig. 6. Two vectors s_i and s_j , embedded in bodies i and j respectively, define a plane perpendicular to the revolute joint axis. In addition, the two vectors define the torsional spring attachment points on the two bodies. The angle between s_i and s_j is denoted by θ . By calculating the instantaneous angle θ , the torque of a torsional spring-damper-actuator element can now be written as

$$b = k_t (\theta - \theta^0) + c_t \dot{\theta} + a_t \quad (23)$$

where k_t , c_t , a_t , and θ^0 are the torsional spring stiffness, damping coefficient, actuator torque, and undeformed angle of the element, respectively.

While the default values of the parameters k , c , θ^0 , a , k_t , c_t , θ^0 , and a_t in Eqs. (22) and (23) are constants, these parameters can be prescribed as general nonlinear functions of the generalized coordinates q , \dot{q} , and the Lagrange multipliers λ . This generality allows for representation of friction in joints, since λ defines reaction force in a joint. Further, general nonlinear springs and dampers can be represented and actuator forces can be used to represent control inputs.

Incorporation of Control and Other Effects

Virtually all modern large-scale mechanical systems involve feedback controllers, hydraulic or electrical actuators, and other interdisciplinary subsystems that interact to influence the dynamics of the system. It is thus important that a usable computer aided analysis formulation explicitly include such effects.

Consider first a feedback control subsystem or a hydraulic subsystem that is described by a set of differential equations of the form

$$\dot{c} = f(q, \dot{q}, c, t) \quad (24)$$

where c is a vector state variable of the controller. The output of the controller is a set of driving forces that can be written as generalized forces contributing to the equations of motion of Eq. (20), i.e.,

$$g^c = g^c(q, \dot{q}, c, t) \quad (25)$$

The form of the force input to the system will, of course, be dependent on the nature of the controller. In particular cases, one may be able to input the control driving effect explicitly as an actuator force or torque in a translational or torsional spring-damper-actuator. This is true for hydraulic rams, hydraulic motors, and electric motors. In such cases, the control actuator force is automatically incorporated into the generalized force vector g by the spring-damper-actuator equations. Similarly, aerodynamic forces, ground-vehicle interface forces, and other forces that depend in a complex way on the kinematic state q and \dot{q} may be incorporated into the model. It is clear that such effects can be routinely incorporated into the formulation, provided that the engineer can write expressions for the forces in terms of q and \dot{q} .

It is important to note that force input to the mechanical system from interdisciplinary effects, represented by Eq. (25), couples the differential equations of motion of Eq. (20) and control equations of Eq. (24). Thus, the system state equations of motion to be integrated include the differential equations of Eqs. (20) and (24), with the control force g^c of Eq. (25) included in g of Eq. (20), the algebraic equations of kinematic constraint of Eq. (13), and a set of initial conditions on q , \dot{q} , and c .

Numerical Integration of System Equations of Motion

Presuming that the m kinematic constraint equations of Eq. (13), written here in the form

$$\Phi(q, t) = 0 \quad (26)$$

are independent, one can use a Gauss-Jordan reduction algorithm with double pivoting⁵ on the Jacobian matrix

$$\Phi_q \equiv \frac{\partial \Phi_i}{\partial q_j} \quad (27)$$

to partition the vector q into $q = [u^T, v^T]^T$, where u are dependent generalized coordinates and v are independent generalized coordinates. The implicit function theorem of calculus¹² guarantees that it is theoretically possible to solve Eq. (26) for $v = v(u)$. In practice, however, an implicit elimination process is used, i.e., when v is fixed, u is determined by Newton-Raphson iteration to solve Eq. (26) for u .

Differentiation of Eq. (26) with respect to time yields the velocity equation

$$\Phi_q \dot{q} = -\dot{\Phi}_t \quad (28)$$

$$\Phi_u \dot{u} + \Phi_v \dot{v} = -\dot{\Phi}_t \quad (29)$$

which can be solved for \dot{u} , once \dot{v} is known, since Φ_u is nonsingular. Note that Φ_u and Φ_v are two matrices made out of the columns of Φ_q corresponding to u and v . Differentiating Eq. (28) with respect to time yields the acceleration equation

$$\Phi_q \ddot{q} = -(\Phi_{qq} \dot{q}) \dot{q} - 2\Phi_{qt} \dot{q} - \ddot{\Phi}_t \quad (30)$$

which are appended to Eq. (20) and then solved for $\ddot{q} = [\ddot{u}^T, \ddot{v}^T]^T$ once the velocities are known. The system dynamic equations may now be solved by applying a predictor-corrector algorithm¹³ to v , \dot{v} , and c as follows:

- 1) Set a time step counter i to $i = 0$, and initialize $t^i = 0$.
- 2) Use initial conditions $q^i = q^0$, $\dot{q}^i = \dot{q}^0$, and $c^i = c^0$.
- 3) Partition q into u and v .
- 4) Solve Eqs. (20) and (30) for \ddot{q}^i and λ^i .
- 5) Select a proper time increment Δt and let $t^{i+1} = t^i + \Delta t$.
- 6) If $t^{i+1} > \text{final time}$ then terminate, otherwise continue.
- 7) Integrate (predictor-corrector) \dot{v}^i , \ddot{v}^i , and c^i to obtain v^{i+1} , \dot{v}^{i+1} , and c^{i+1} , respectively.
- 8) Increment i to $i + 1$.
- 9) Knowing v^i from 7), solve Eq. (26) for u^i .
- 10) Knowing \dot{v}^i from 7), solve Eq. (29) for \dot{u}^i .
- 11) Knowing c from 7) solve Eq. (24) for \dot{c} .
- 12) Determine g^c from Eq. (25) and include in g of Eq. (20).
- 13) Go to 4.

The use of Cartesian and Euler parameter-generalized coordinates yields a maximal set of loosely coupled nonlinear holonomic constraints and differential equations of motion. A Gaussian elimination algorithm with full pivoting decomposes the constraint Jacobian matrix and automatically identifies dependent and independent generalized coordinates.

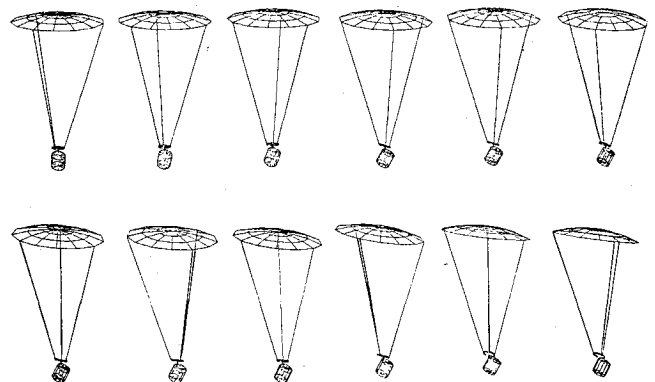


Fig. 8 Animation of parachute descending in air.

The constraint Jacobian matrix is sparse; thus the algorithm provides the necessary information to establish a modified sparse matrix relating variations in dependent and independent variables. Sparse matrix algorithms with symbolic factorization are used to carry out the repetitive numerical solution of matrix equations required in the algorithm efficiently. For more detail on this numerical algorithm and its implementation, see Ref. 5. General purpose computer programs, called the Dynamic Analysis and Design System (DADS), have been developed to implement the foregoing algorithm for planar (DADS-2D) and spatial (DADS-3D) systems. All the algebraic and differential equations are automatically assembled by the programs from input data describing the system. Additional nonstandard constraints, interdisciplinary force inputs, and control differential equations can be provided through user supplied subroutines.

Examples

Three examples of mechanical systems incorporating interdisciplinary effects are presented here in summary form. Dynamic response of each system studied is illustrated through use of a sequence of graphical snapshots that provides a crude animation of system dynamics. With modern high-speed computer graphics devices, an animation with 30

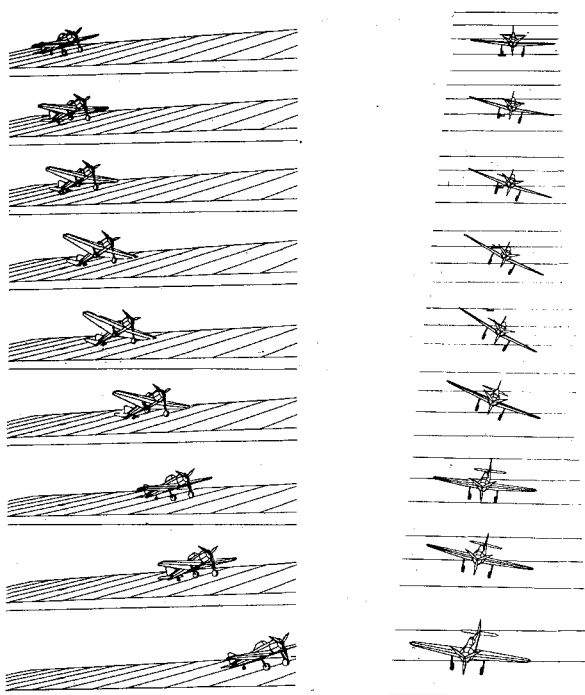


Fig. 9 Animation of aircraft landing from side and front views.

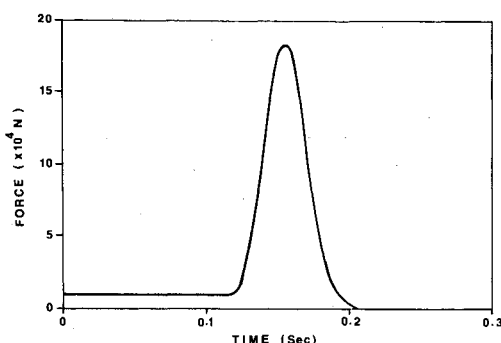


Fig. 10 Total reaction force acting on landing gear of a wheel transversing an obstacle.

frames per second can be obtained to assist in visualization and unstanding of system performance.

Parachute

Figure 7 illustrates a model of a 27 degree-of-freedom spinning parachute. A relatively heavy package is attached to a circular plate by two small links. Three revolute joints connect the plate, links, and the package. The canopy is modeled by three rigid panels having a common point, modeled by two spherical joints. The panels are connected to each other and to the plate by several strings. The strings are modeled by nonlinear translational spring dampers in which spring stiffness is described as a function of the distance between its two attachment points. When this distance is less than the undeformed string length, the spring constant is zero; when the distance is equal or greater than the length, the spring constant becomes large. Aerodynamic forces, functions of parachute descent velocity, altitude, and attitude act on the canopy. User supplied subroutines are provided to compute the aerodynamic forces and torques defined relative to the panel coordinate systems. The aerodynamic forces are then converted to the global coordinate system. The torques are converted to the Euler parameter system, and are then added to the vector of generalized forces. The simulation demonstrates that the aerodynamic forces impact spin and precession action to the canopy. When friction is included between the circular plate and the attached link, the rest of the model follows the spin action of the canopy and the plate. An animation of the dynamic response of the system is given in Fig. 8.

Aircraft on Damaged Runway

A small single-engine aircraft moving on a damaged runway was simulated using arbitrary data, by considering the main body and the wings to be rigid. The wheels were modeled as separate bodies connected to the landing gear by revolute joints. The runway was modeled as a flat surface with obstacles such as bumps or potholes, where the height (depth) and diameter of the obstacle were varied from one simulation to another. It was assumed that the aircraft was moving with a constant speed on the runway before encountering the obstacle. Figure 9 illustrates the response of one of the simulations graphically. The Lagrange multipliers associated with the constraint equations of the revolute joints determine the reaction forces at the joints. Figure 10 shows the total reaction force acting on the landing gear of the wheel crossing the obstacle. Such information is valuable in design of aircraft for use in severe landing environments.

Truck With Flexible Chassis

In the formulation of kinematic constraints and equations of motion discussed in the previous sections, it was assumed that all bodies in a given system are rigid. Recently, another version of the DADS code was developed that can treat deformable bodies as well as rigid bodies.^{8,14} Multibody systems consisting of interconnected rigid and flexible sub-

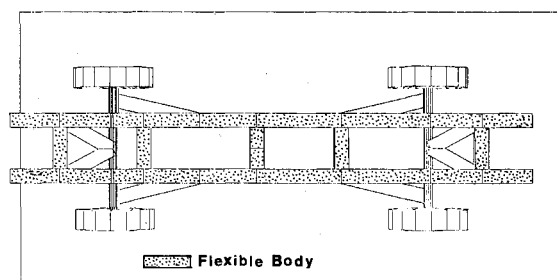


Fig. 11 Truck model with flexible chassis.

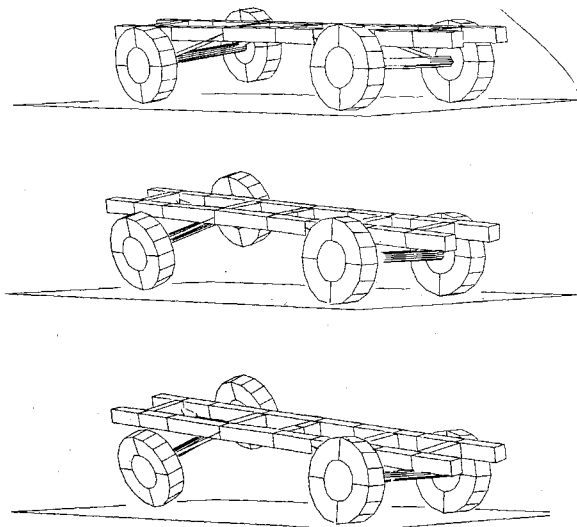


Fig. 12a Animation of truck simulation: chassis response.

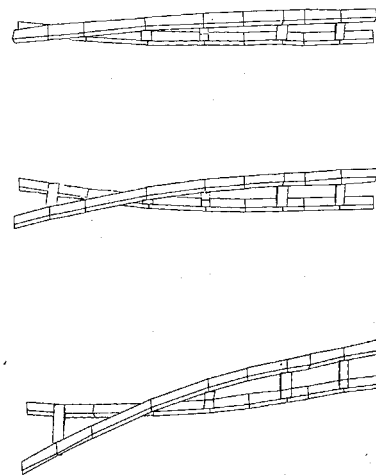


Fig. 12b Animation of truck simulation: chassis deformation magnified 50 times.

structures, which may undergo large angular rotation and translation, can be analyzed. Initially the finite element method is used to characterize the elastic properties of deformable substructures. A component mode technique is then employed to eliminate insignificant substructure modes. Nonlinear holonomic constraint equations are used to couple substructure physical and modal equations of motion. The method of solving the complete set of algebraic and differential equations of motion is the same as the method discussed in this paper for purely rigid body dynamic analysis.

A truck model with a flexible chassis is shown in Fig. 11 to illustrate interconnected flexible and rigid body dynamic analysis.¹⁴ The chassis, which is modeled as a flexible body as shown in Fig. 11, is connected to the rear and front axles by eight rigid links. The suspension system is presented by four springs connected between axles and chassis. Elastic characteristics of the tires are also considered in the model. The flexible chassis is divided into 24 beam elements. An eigenvalue problem is solved for vibration of the chassis and ten significant modes are considered for dynamic analysis.

The source of excitation to the model is a 1-m-high ramp passing beneath the right front wheel in 3 s. An animation of the response simulation is shown in Fig. 12a, where the ramp is not shown. Chassis deformation is magnified 50 times and shown in Fig. 12b.

Conclusion

The computer based method presented in this paper is applicable to a wide range of dynamic systems with multidisciplinary effects. The examples presented illustrate that systems with mixed rigid and flexible bodies can be analyzed for dynamic response. Highly nonlinear phenomena, such as aerodynamic forces, feedback control, wheel-ground interface, etc., can be included in the model. Therefore, dynamic response of an aircraft, as an example of mixed rigid and flexible bodies under aerodynamic loading, can be modeled and studied. Similarly, deployable space structures that undergo spatial motion can be analyzed.

Animated graphics has proved to be a powerful tool for dynamic response visualization. It provides the analyst with the means to comprehend the nature of the motion rather easily. Many interesting aspects of a motion predicted by a dynamic analysis may be revealed before an attempt to study a plot or a listing of the response for more extensive information is made.

References

- ¹Chace, M.A. and Smith, D.A., "DAMN-A Digital Computer Program for the Dynamic Analysis of Generalized Mechanical Systems," SAE Paper 71024, 1971.
- ²Paul, B. and Krajcinovic, D., "Computer Analysis of Machines with Planar Motion—Part I: Kinematics; Part II: Dynamics," *Journal of Applied Mechanics*, Vol. 37, 1970, p. 697.
- ³Sheth, P.N. and Uicker, J.J. Jr., "IMP (Integrated Mechanisms Program), A Computer Aided Design Analysis System for Mechanisms and Linkages," *Journal of Engineering for Industry*, Vol. 94, 1972, p. 454.
- ⁴Orlande, N., Chace, M.A., and Calahan, D.A., "A Sparsity-Oriented Approach to the Dynamic Analysis and Design of Mechanical Systems, Parts I and II," *Journal of Engineering for Industry*, Vol. 99, 1977, p. 773.
- ⁵Wehage, R.A. and Haug, E.J., "Generalized Coordinate Partitioning for Dimension Reduction in Analysis of Constrained Dynamic Systems," *ASME Journal of Mechanical Design*, Vol. 104, No. 1, 1982, p. 247.
- ⁶Nikravesh, P.E. and Chung, I.S., "Application of Euler Parameters to the Dynamic Analysis of Three Dimensional Constrained Mechanical Systems," *ASME Journal of Mechanical Design*, Vol. 104, No. 4, Oct. 1982.
- ⁷Song, J.O. and Haug, E.J., "Dynamic Analysis of Flexible Mechanisms," *Computer Methods in Applied Mechanics and Engineering*, Vol. 24, 1980, p. 359.
- ⁸Shabana A. and Wehage, R.A., "Variable Degree-of-Freedom Component Mode Analysis of Inertia Variant Mechanical Systems," *ASME Journal of Mechanics Transmission and Automation in Design*, Vol. 105, No. 3, Sept. 1983.
- ⁹Nikravesh, P.E. and Haug, E.J., "Generalized Coordinate Partitioning for Analysis of Mechanical Systems with Nonholonomic Constraints," *ASME Journal of Mechanics Transmission and Automation in Design*, Vol. 105, No. 3, Sept. 1983, pp.
- ¹⁰Wittenburg, J., *Dynamics of Systems of Rigid Bodies*, Teubner, Stuttgart, 1977.
- ¹¹Goldstein, H., *Classical Mechanics*, Addison-Wesley, Reading, Mass., 1980.
- ¹²Hildebrand, F.B., *Advanced Calculus for Applications*, Prentice-Hall, Englewood Cliffs, N.J., 1976.
- ¹³Shampine, L.F. and Gordon, M.K., *Computer Solution of Ordinary Differential Equations: The Initial Value Problem*, W.J. Freeman, San Francisco, Calif., 1975.
- ¹⁴Shabana, A. and Wehage, R.A., "Dynamic Analysis of Large Scale Inertia-Variant Flexible Systems," Report No. 82-7, Center for Computer Aided Design, University of Iowa, Iowa City, Ia., 1982.